Hindawi Publishing Corporation
Journal of Materials
Volume 2014, Article ID 642069, 5 pages
http://dx.doi.org/10.1155/2014/642069

Research Article

Electrochemical Behavior of TiO_2 Nanoparticle Doped WO_3 Thin Films

Suvarna R. Bathe[1,2] and P. S. Patil[2]

[1] *Polymer and Functional Materials Division, CSIR-Indian Institute of Chemical Technology (IICT), Hyderabad 500607, India*
[2] *Thin Films Material Laboratory, Physics Department, Shivaji University, Kolhapur 416004, India*

Correspondence should be addressed to Suvarna R. Bathe; bathesr@gmail.com

Received 30 December 2013; Accepted 6 April 2014; Published 6 May 2014

Academic Editor: Israel Felner

Nanoparticle TiO_2 doped WO_3 thin films by pulsed spray pyrolysis technique have been studied on fluorine tin doped (FTO) and glass substrate. XRD shows amorphous nature for undoped and anatase phase of TiO_2 having (101) plane for nanoparticle TiO_2 doped WO_3 thin film. SEM shows microfibrous reticulated porous network for WO_3 with 600 nm fiber diameter and nanocrystalline having size 40 nm for TiO_2 nanoparticle doped WO_3 thin film. TiO_2 nanoparticle doped WO_3 thin film shows ~95% reversibility due to may be attributed to nanocrystalline nature of the film, which helpful for charge insertion and deinsertion process. The diffusion coefficient for TiO_2 nanoparticle doped WO_3 film is less than undoped WO_3.

1. Introduction

The electrochromism is key to green technology as it controls the energy of solar flux entering in building, utilizes solar energy, and increases comfort in buildings. Electrochromic materials are able to sustain reversible and persistent changes of their optical properties under the action of a voltage. The electrochromic phenomenon was discovered in tungsten oxide [1] and this material remains the most promising candidate for large-scale uses of electrochromic devices. Their potential applications include several technological areas, such as smart windows, self-dimming rear mirror, electrochromic display, and antiglare rear view mirrors of automobiles [2]. Among a variety of the transition metal oxides, tungsten oxide (WO_3-x) is found to be the most efficient candidate for electrochromic applications. Granqvist [3] explains the theoretical explanation of electrochromic mechanism and reviews about different nanostructured oxides for electrochromic device and describes the mass fabrication by electrochromic foil technology. The electrochromic performance of tungsten oxide, reversible coloration under double injection of ions and electrons, strongly depends on its nature and microstructure. Nanoscale microstructure could improve the electrochromic performances of tungsten oxide thin film because it is easy for ion to intercalate and deintercalate in thin film. Mesoporous tungsten oxides exhibit superior high-rate ion-insertion performance for their short-diffusion length of lithium and hydrogen ions into electrochromic films [4]. Several researchers have attempted to employ the concept of nanotechnology to improve the drawbacks of thin-film-based electrochromic devices (ECDs) such as contrast, cycling life stability, and slow switching time between the colored and bleached states. The researcher developed transition metal oxide nanowires based ECDs that show a great improvement in coloration efficiency, contrast, and durability [5, 6]. These ECDs show promising switching rate, life stability, and contrast. Grätzel [7] used TiO_2 nanoparticles and absorbed organic monomers to improve the switching speed. The coloration and bleaching rates of WO_3 film increase with the addition of the porous conducting metallic cover layer in a liquid electrolyte cell [8]. Park [9] has studied electrochromic properties of cosputtered Au-WO_3 nanocomposite thin films containing high gold concentration (60 mol% Au) and obtained a shorter response time relative

to the pure WO_3 thin film. The doping of Au nanocrystals in WO_3 thin films shows fast coloration time which was ten times shorter as compared with the coloration time of the pure WO_3 thin film [10]. Some literature is available on WO_3 films doped with Co, Cr, and Ni for electrochromic properties for ECD [11, 12]. He et al. [13] showed that the addition of gold over layer on WO_3 thin film formed by physical vapor deposition resulted in a better change of optical density in electrochromic process. Previously our lab studied [14, 15] gold nanoparticles, multiwalled carbon nanotube doped in the WO_3 thin films by pulsed spray for improving EC properties. The small doping of Ni (0.3 at %) in WO_3 thin films improves electrochromic property, but EC property vanishes due to the limited ion diffusivity for higher concentration [16]. The effects of molybdenum (Mo) doping on the electrochromic behavior of spray pyrolyzed tungsten trioxide [WO_3] thin films have been studied [17]. Our earlier work of Ti and Nb doping in WO_3 thin films by pulsed spray pyrolysis shows with improved EC properties, but coloration efficiency decreases [18, 19]. Very little literature is available on TiO_2 nanoparticle WO_3 thin films. The main goal is to increase coloration efficiency by TiO_2 nanoparticle doping in WO_3 matrix.

2. Experimental Details

The undoped and TiO_2 nanoparticle doped WO_3 thin films were grown on fluorine doped tin oxide (SnO_2 : F, FTO) coated glass and microscopic glass substrates using pulsed spray pyrolysis deposition technique. The precursor solution used for deposition of the films was prepared by dissolving pure WO_3 powder in ammonia and distilled water and then heated to 90°C (prior to spray) at which the formation of ammonium tungstate ($(NH_4)_2WO_4$) is completed. Commercial TiO_2 nanoparticle (average particle size ~25 nm) 4 mg is dissolved in 5 mL trioctylphosphine oxide (TOPO) and stirred for 15 minutes; then, ammonium tungstate was added slowly to this solution. Details of the films synthesis are described elsewhere [20]. In brief, the substrate was held at 250°C, while an airflow rate of 15 L/min was maintained during deposition. The solution spraying on and off time interval was kept 5 s (50% duty cycle) for both cases. The thickness of all deposited films was about 200 nm. After deposition, the films were annealed in air at 325°C for 0.5 h.

The structural properties were studied using an X-ray diffractometer (XRD) with Cu K_α radiation of wavelength 1.542 Å. X-ray diffraction data were used to identify the phases present in the films and to find out changes in the lattice parameters, if any. The surface morphology of the films was studied using scanning electron microscopy. The optical measurements were carried out at room temperature using a UV-VIS-NIR spectrophotometer. The transmittance of the films was measured in a wavelength range 200–3000 nm. The electrochemical injection or extraction of electrons and H^+ ions was carried out using a solution of 0.001 M of H_2SO_4 electrolyte solution with platinum as a counter electrode and saturated calomel as a reference electrode (SCE). It was confirmed that our data for the undoped films compare very well with the best results reported by other groups [3, 8, 10–12, 21]. This ensures the quality of our films processing conditions and procedures.

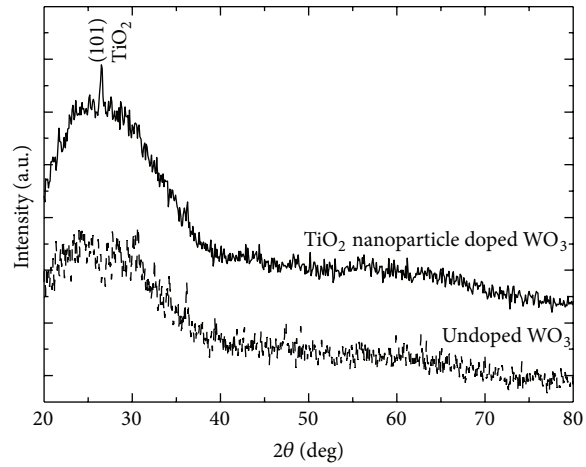

Figure 1: XRD of undoped and TiO_2 nanoparticle doped WO_3 thin films.

3. Results and Discussion

The X-ray diffraction patterns of the undoped and TiO_2 nanoparticle doped WO_3 thin films deposited on glass substrate are shown in Figure 1. The XRD pattern for undoped WO_3 films shows no distinct diffraction peaks, indicating the amorphous nature. The boards hump at diffraction angle ~20–30 degrees is originating from glass substrate. In case of TiO_2 nanoparticle doped WO_3 films, one peak at $d = 3.346$ Å is observed, which indexed as (101) of anatase phase of TiO_2 in accordance with JCPDS-ICDD card number 75-1537.

The morphology for the undoped and TiO_2 nanoparticle doped WO_3 films was examined using SEM. Figure 2(a) shows SEM image for undoped WO_3 film deposited at 250°C and annealed at 325°C on glass substrate. It clearly shows microfibrous reticulated surface morphology throughout the film. The film appears to be of a multilayered fibrous nature, with mean fiber diameters of about 600 nm. This morphology is helpful for ion intercalation and deintercalation of the film. Figure 2(b) shows the SEM image of TiO_2 nanoparticle doped WO_3 thin films. TiO_2 nanoparticle doping ruptures WO_3 fibrous reticulate network and TiO_2 nanoparticles were segregated in the surface of the film to form large clusters with particle size ~40 nm.

Cyclic voltammograms (CV) were recorded for all the undoped and TiO_2 nanoparticle doped films with linear potential sweep between −500 and +500 mV at a scan rate of 50 mV/s and shown in Figure 3. The arrow indicates the scan direction. When a negative potential was applied, a blue color was observed, indicating the oxide reduction followed by H^+ ions intercalation. After the reversal of the potential, the anodic current started to flow, corresponding to the deintercalation process. There is a well-defined anodic peak for the film, indicating that the H^+ insertion-removal process is highly reversible with little hysteresis. The area of the hysteresis curves and the height and position of anodic

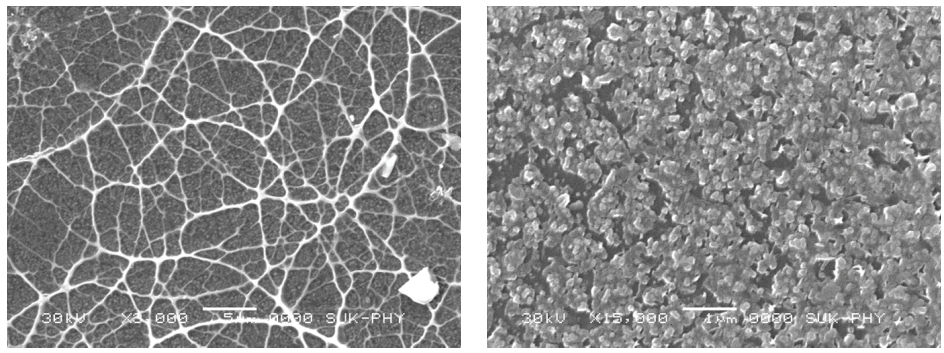

(a) (b)

Figure 2: SEM images for (a) undoped and (b) TiO_2 nanoparticle doped WO_3 thin films.

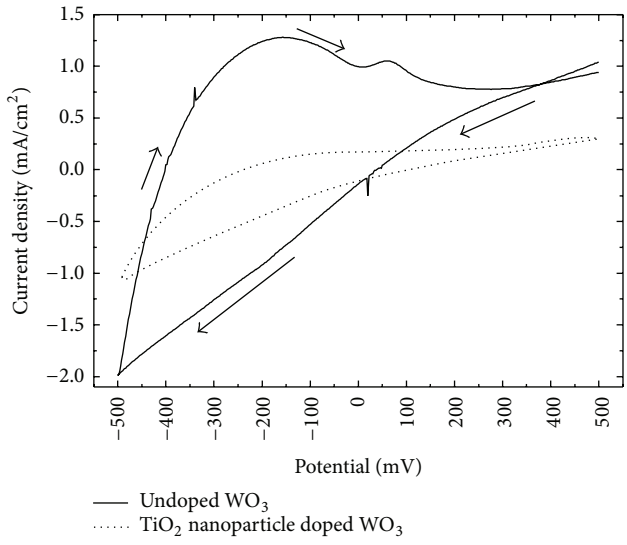

Figure 3: Cyclic voltammograms (CV) for undoped and TiO_2 nanoparticle doped WO_3 thin films.

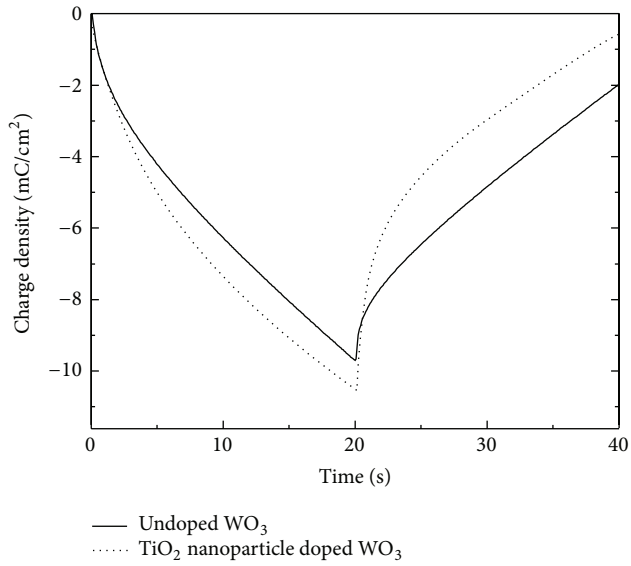

Figure 4: Chronocoulometry (CC) for undoped and TiO_2 nanoparticle doped WO_3 thin films, recorded at potential step ±0.5 V for 20 s.

and cathodic peaks are closely related to the electrochemical processes occurring in the WO_3. The decrease in the area of voltammograms and shift of threshold voltage (E_Γ) towards positive potential (from −48 to +63 mV) is observed in case of TiO_2 nanoparticle doped WO_3 films as compared to undoped WO_3 films. This can be attributed to decrease in ion mobility of the TiO_2 nanoparticle doped WO_3 thin films.

The diffusion coefficient (D) of H^+ ions during intercalation and deintercalation is calculated by using Randles-Sevcik equation [22]:

$$D^{1/2} = \frac{j_p}{2.72 \times 10^5 \times n^{3/2} \times A \times C_0 \nu^{1/2}}, \quad (1)$$

where j_p is the peak current density (anodic peak current density (j_{pa}) and cathodic peak current density (j_{pc})), n is number of electron, C_0 is the concentration of active ions in the solution, ν is the scan rate, and A is the film area. By substituting all the values, the diffusion coefficient at 50 mV/s scan rate is calculated for intercalation and deintercalation processes for the undoped and TiO_2 nanoparticle doped films. The diffusion coefficient is 1.86×10^{-9} and 1.38×10^{-11} cm^2/s for the undoped and TiO_2 nanoparticle doped films, respectively. This indicates that the charge insertion of TiO_2 nanoparticle doped WO_3 films is less than undoped thin film.

The amount of H^+ ions intercalation and deintercalation with respect to time was carried by using chronocoulometry (CC) studies, which can further be used to estimate reversibility and coloration efficiency. Figure 4 shows charges intercalated/deintercalated versus time transients for the films at ±0.5 V for the step of 20 seconds. In the forward scan, the charges are intercalated into the film by diffusion resulting process in coloration due to reduction of W^{+6} to W^{+5} states. In the reverse scan, the intercalated charge is removed from the film, resulting in bleaching due to oxidation of W^{+5} to W^{+6} states. The reversibility of the films is calculated by the ratio of charge deintercalated (Q_{di}) from the film into

Table 1: The electrochromic properties of undoped and TiO_2 nanoparticle doped WO_3 films.

Sample ID	Q_i (mC/cm^2)	Q_{di} (mC/cm^2)	(ΔOD) (%)	Reversibility (%)	CE (cm^2/C) at 630 nm	Diffusion coefficient (cm^2/s)
Undoped WO_3	9.71	7.12	0.14	75	30	1.86×10^{-9}
TiO_2 nanoparticle doped WO_3	10.60	9.98	0.02	95	2	1.38×10^{-11}

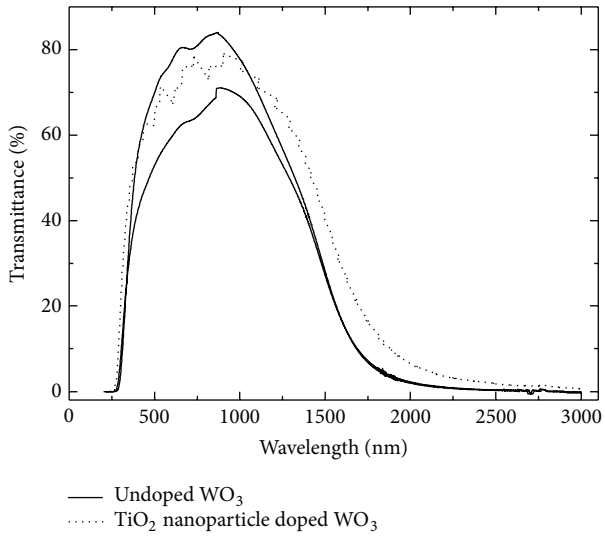

Figure 5: Optical transmittance for the bleached (up curve) and the colored (down curve) for undoped (solid line) and TiO_2 nanoparticle doped (dotted line) WO_3 films.

electrolyte to the charge intercalated (Q_i) into the film from the electrolyte. The electrochromic reversibility was found to be ~75% for undoped WO_3 and 95% for TiO_2 nanoparticle doped WO_3 films. The electrochromic properties calculated from CV and CC were listed in Table 1.

The dependence of optical transmittance on wavelength in the 200–3000 nm for the undoped and TiO_2 nanoparticle doped WO_3 films in bleached and colored condition for 10 sec is shown in Figure 5. The maximum transmittance observed was ~80% at 860 nm and ~75% at 910 nm for undoped and TiO_2 nanoparticle doped WO_3 films in bleached state, respectively. All the colored films show similar trend as in bleached films; the only difference is that the maximum transmittance value decreases as compared to the respective bleached films. The undoped and TiO_2 nanoparticle doped WO_3 films exhibit above ~50% optical transmission in the ~400–1300 nm range and drop abruptly beyond ~1600 nm. The drop in transmission in near infrared (NIR) region can be attributed to an increased reflectance of the films in NIR region [21, 23]. The coloration efficiency (η) at a particular wavelength correlates with the optical contrast, that is, the change in optical density (ΔOD) with charges intercalated per unit electrode area (Q_i), and can be expressed as

$$\eta = \frac{\Delta \mathrm{OD}_\lambda}{Q_i} = \frac{\log\left(T_b/T_c\right)}{Q_i}, \quad (2)$$

where T_b and T_c are the transmittances of the film in the bleached and colored states, respectively. The coloration efficiency decreases in the case of TiO_2 nanoparticle doped WO_3 films, as expected, indicating that Ti does not take part in the electrochromism mechanism. The values of coloration efficiency at 630 nm for 10 sec are calculated using the above equation for the undoped and TiO_2 nanoparticle doped WO_3 films and listed in Table 1.

4. Conclusion

In conclusion, TiO_2 nanoparticles doping effects on electrochromic WO_3 films synthesized using pulsed spray pyrolysis deposition technique have been investigated. The fibrous reticulated morphology is converted into granular structure at TiO_2 nanoparticle doping. The TiO_2 particulates were segregated on the surface of the film, for doped film. It is seen that TiO_2 nanoparticles doping can lead to significant surface morphology changes, which plays an important role in electrochromic properties of WO_3 thin films. It was found that the coloration efficiency decreased in case of TiO_2 nanoparticles doped films. This indicates that the charge inserted into TiO_2 nanoparticle doped WO_3 thin film is not sufficient for reducing tungsten species and also observed diffusion coefficient for this film is about ten times less than undoped WO_3 films.

Conflict of Interests

The authors declare that there is no conflict of interests regarding the publication of this paper.

References

[1] S. K. Deb, "A novel electrophotographic system," *Applied Optics*, vol. 8, supplement 1, pp. 192–195, 1969.

[2] P. M. S. Monk, R. J. Mortimer, and D. R. Rosseinsky, *Electrochromism: Fundamentals and Applications*, VCH, Weinheim, Germany, 1995.

[3] C. G. Granqvist, "Oxide electrochromics: an introduction to devices and materials," *Solar Energy Materials and Solar Cells*, vol. 99, pp. 1–13, 2012.

[4] E. O. Zayim, P. Liu, S.-H. Lee et al., "Mesoporous sol-gel WO_3 thin films via poly(styrene-co-allyl-alcohol) copolymer templates," *Solid State Ionics*, vol. 165, no. 1–4, pp. 65–72, 2003.

[5] C. C. Liao, F. R. Chen, and J. J. Kai, "WO_{3-x} nanowires based electrochromic devices," *Solar Energy Materials and Solar Cells*, vol. 90, no. 7-8, pp. 1147–1155, 2006.

[6] K. C. Cheng, F. R. Chen, and J. J. Kai, "V_2O_5 nanowires as a functional material for electrochromic device," *Solar Energy Materials and Solar Cells*, vol. 90, no. 7-8, pp. 1156–1165, 2006.

[7] M. Grätzel, "Materials science: ultrafast colour displays," *Nature*, vol. 409, pp. 575–576, 2001.

[8] A. R. Haranahalli and P. H. Holloway, "The influence of metal overlayers on electrochromic behavior of WO_3 films," *Journal of Electronic Materials*, vol. 10, no. 1, pp. 141–172, 1981.

[9] K. W. Park, "Electrochromic properties of Au-WO_3 nanocomposite thin-film electrode," *Electrochimica Acta*, vol. 50, no. 24, pp. 4690–4693, 2005.

[10] N. Naseri, R. Azimirad, O. Akhavan, and A. Z. Moshfegh, "Improved electrochromical properties of sol-gel WO_3 thin films by doping gold nanocrystals," *Thin Solid Films*, vol. 518, no. 8, pp. 2250–2257, 2010.

[11] P. K. Shen, J. Syed-Bokhari, and A. C. C. Tseung, "Performance of electrochromic tungsten trioxide films doped with cobalt or nickel," *Journal of the Electrochemical Society*, vol. 138, no. 9, pp. 2778–2783, 1991.

[12] S. K. Deb, S. H. Lee, C. E. Tracy, J. R. Pitts, B. A. Gregg, and H. M. Branz, "Stand-alone photovoltaic-powered electrochromic smart window," *Electrochimica Acta*, vol. 46, no. 13-14, pp. 2125–2130, 2001.

[13] T. He, Y. Ma, Y. Coa, W. Yang, and J. Yoa, "Enhanced electrochromism of WO_3 thin film by gold nanoparticles," *Journal of Electroanalytical Chemistry*, vol. 514, no. 1-2, pp. 129–132, 2001.

[14] P. M. Kadam, N. L. Tarwal, S. S. Mali, H. P. Deshmukh, and P. S. Patil, "Enhanced electrochromic performance of f-MWCNT-WO_3 composite," *Electrochimica Acta*, vol. 58, no. 1, pp. 556–561, 2011.

[15] P. M. Kadam, N. L. Tarwal, P. S. Shinde et al., "Enhanced optical modulation due to SPR in gold nanoparticles embedded WO_3 thin films," *Journal of Alloys and Compounds*, vol. 509, no. 5, pp. 1729–1733, 2011.

[16] S. V. Green, E. Pehlivan, C. G. Granqvist, and G. A. Niklasson, "Electrochromism in sputter deposited nickel-containing tungsten oxide films," *Solar Energy Materials and Solar Cells*, vol. 99, pp. 339–344, 2012.

[17] J. M. O. R. de León, D. R. Acosta, U. Pal, and L. Castañeda, "Improving electrochromic behavior of spray pyrolised WO_3 thin solid films by Mo doping," *Electrochimica Acta*, vol. 56, no. 5, pp. 2599–2605, 2011.

[18] S. R. Bathe and P. S. Patil, "Titanium doping effects in electrochromic pulsed spray pyrolysed WO_3 thin films," *Solid State Ionics*, vol. 179, no. 9-10, pp. 314–323, 2008.

[19] S. R. Bathe and P. S. Patil, "Influence of Nb doping on the electrochromic properties of WO_3 films," *Journal of Physics D*, vol. 40, no. 23, pp. 7423–7431, 2007.

[20] S. R. Bathe and P. S. Patil, "Electrochromic characteristics of fibrous reticulated WO_3 thin films prepared by pulsed spray pyrolysis technique," *Solar Energy Materials and Solar Cells*, vol. 91, no. 12, pp. 1097–1101, 2007.

[21] M. Deepa, A. K. Srivastava, and S. A. Agnihotry, "Influence of annealing on electrochromic performance of template assisted, electrochemically grown, nanostructured assembly of tungsten oxide," *Acta Materialia*, vol. 54, no. 17, pp. 4583–4595, 2006.

[22] A. J. Bard and L. R. Faulkner, *Electrochemical Methods*, Wiley-Interscience, New York, NY, USA, 1980.

[23] F. O. Arntz, R. B. Goldner, B. Morel, T. E. Hass, and K. K. Wong, "Near-infrared reflectance modulation with electrochromic crystalline WO_3 films deposited on ambient temperature glass substrates by an oxygen ion-assisted technique," *Journal of Applied Physics*, vol. 67, no. 6, pp. 3177–3179, 1990.